

Mössbauer Effect with Ni^{61}

FELIX E. OBENSHAIN AND HORST H. F. WEGENER*

Oak Ridge National Laboratory, Oak Ridge, Tennessee

(Received October 21, 1960)

The Mössbauer effect is observed in Ni^{61} . The Ni^{61*} was obtained by $\text{Ni}^{64}(p,\alpha)\text{Co}^{61} \xrightarrow{\beta^- (99 \text{ min})} \text{Ni}^{61*}$, giving a nickel Mössbauer nucleus in a Ni^{64} host lattice. The magnitude of the effect at $T=80^\circ\text{K}$ is about 4% for a 400 mg/cm^2 absorber foil (natural nickel). From the thickness dependence we obtain $f_{\text{source}}=f_{\text{abs}}=(9\pm1)\%$ for the Debye-Waller factor at $T=80^\circ\text{K}$. The temperature dependence yields a Debye temperature varying between 413° and 437° . The velocity dependence has a half-width of 1.65 mm/sec . The spectrum deviates from the Lorentz shape expected for a single line. A recent electronic determination of the lifetime of this 71-kev state indicates a natural half-width of 0.37 mm/sec . The increased half-width and shape of the spectrum observed in our experiment may be understood in terms of a magnetic hyperfine splitting. The moment of the ground state is known. The internal field H and the magnetic moment μ_e of the first excited state are unknown. An analysis of the data gives a connection between the two quantities, $\mu_e(H)$.

I. INTRODUCTION

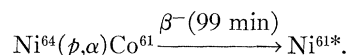
THE most interesting nucleus available for the Mössbauer effect so far, is probably Fe^{57} . Because iron belongs to the ferromagnetic metals, many nice experiments were possible: determination of nuclear moments, internal fields, etc.¹ There exists yet another ferromagnetic nucleus, Ni^{61} , with Mössbauer properties: stable isotope, 71-kev excited state with a reasonable lifetime, low internal conversion, and high Debye temperature. Surprisingly, this nucleus is not listed in Nagle's "Table of Mössbauer Candidates" (reference 1). There are, of course, some possibilities of producing the 71-kev state of Ni^{61} : Coulomb excitation, β^- decay (Co^{61} , $T_{1/2}=99 \text{ min}$) and β^+ decay (Cu^{61} , $T_{1/2}=200 \text{ min}$). In spite of the relative short half-life of Co^{61} we have chosen the β^- decay. The β^+ decay is connected with a high gamma-ray background. The Coulomb excitation has some problems of a solid-state nature (e.g., knocking out of the atom from the lattice site), which have not been solved yet.

The Ni^{61} states involved (Fig. 1) have closed proton shells. There are five neutrons in the $p_{3/2}$ and $f_{7/2}$ levels outside the closed 28 shell. The 71-kev state may be

understood as a single-neutron state ($f_{7/2}$). In the ground state $(p_{3/2})^{-1}(f_{7/2})^2$ one of the $p_{3/2}$ neutrons is lifted to the $f_{7/2}$ level (pairing energy). The 71-kev γ radiation is an $M1$ transition (see Sec. V). An $M1$ -transition $p_{3/2} \rightarrow f_{7/2}$ is l forbidden. In agreement with this prediction, the measured transition probability is, indeed, much smaller (about $1/100$) than l -allowed $M1$ single particle transitions of the same energy. This single-particle situation allows some statements about the magnetic moment of the excited state.

II. PROCEDURE

Mössbauer experiments may best be understood if the host lattice of the source is of the same kind as the nucleus emitting the resonant radiation. In order to obtain the excited state of Ni^{61} in a nickel lattice, 95% enriched Ni^{64} was bombarded in the ORNL 86-in. cyclotron. The proton energy of this cyclotron is about 22 Mev. The reaction is



The Ni^{64} was electroplated² (for example, 40 mg/3 cm^2) on an aluminum backing. The cyclotron bombarding time and beam current were chosen so that a maximum

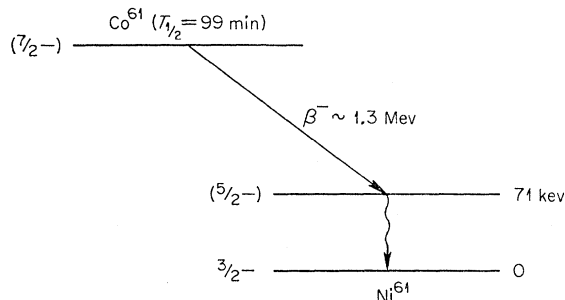


FIG. 1. The pertinent nuclear data are indicated in the diagram. The lifetime of the 71-kev state is now known: $T_{\text{mean}} = (7.6 \pm 0.7) \times 10^{-9} \text{ sec}$.

* On leave from University of Erlangen, Erlangen, Germany.

¹ Mössbauer Effect Conference, University of Illinois, Urbana, Illinois, June, 1960, edited by H. Frauenfelder and H. Lustig.

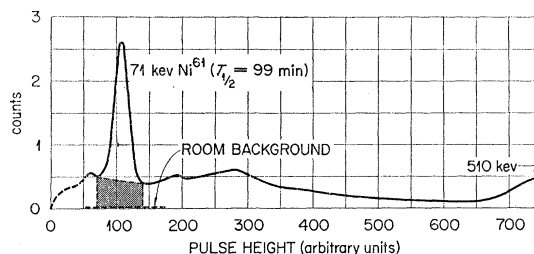


FIG. 2. The spectrum shown was obtained 40 min after irradiation in the cyclotron. The 71-kev gamma ray is the only prominent gamma ray. The background is taken as the shaded area. The spectrum was measured at intervals of 30 min.

² See, for example, *Modern Electroplating*, edited by A. G. Gray (John Wiley & Sons, Inc., New York, 1953).

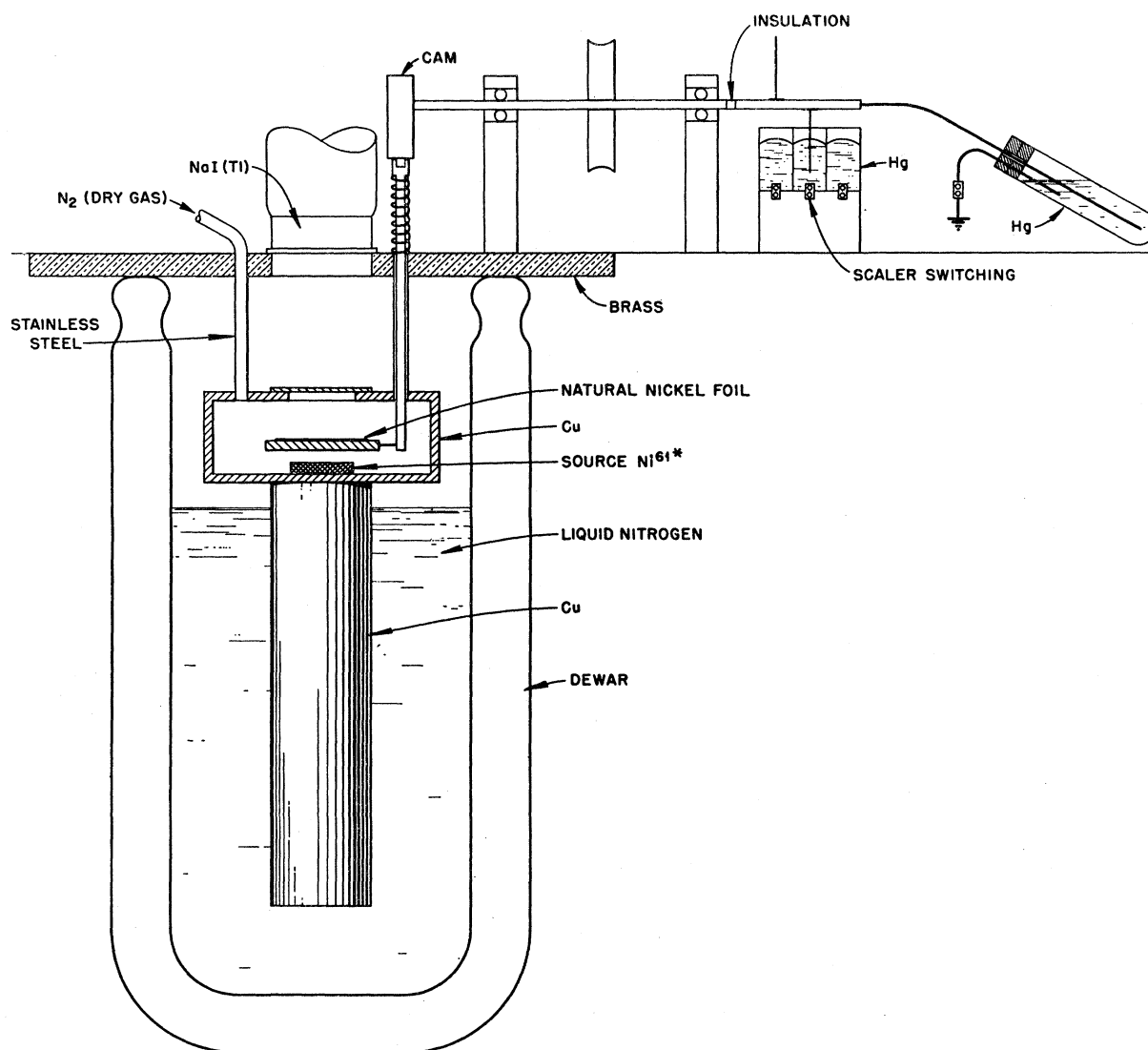


FIG. 3. A schematic diagram of the equipment used in this experiment shows the relative orientation of the source, absorber foil, and gamma detector. A synchronous motor, not shown, is used to drive the cam. The coupling is an O-ring belt.

of 10^4 counts/sec would be observed for our geometry. Cleanliness of the source is clearly demonstrated in Fig. 2; the predominate line is the 71-kev gamma. After bombarding the Ni^{64} with 22-Mev protons, a sizable fraction of the Co^{61} nuclei should be displaced from normal lattice sites. In order to repair such radiation damage, the source was heated to 500°C for five minutes. The absorber foils used throughout this experiment were natural nickel (1.25% Ni^{61}). The largest foil thickness used was 825 mg/cm^2 .

The probability, f , for recoil-free gamma emission, computed on the basis of the Debye model, suggested that the measurements could be done at liquid nitrogen temperature. The source and absorber were located in the same low-temperature bath and the absorber was moved relative to the source.

III. APPARATUS

The copper chamber shown in Fig. 3 served as a low-temperature cavity and contained the source and absorber. The liquid nitrogen was contained in an ordinary Dewar flask. The area within the chamber was kept free of ice by circulating dry nitrogen gas through it. Measurements using a copper-constantan thermocouple showed that the source and absorber could be maintained at temperatures between 77°K and 80°K without difficulty. Insulation of the copper chamber from room temperature was obtained by means of thin stainless steel tubes extending down from the brass cover plate. The absorber was supported on a Lucite ring attached to a stainless steel tube.

A shaped cam determined the motion of the absorber foil attached to a push rod. The cam was coupled to a

continuously variable mechanical speed reducer and a synchronous motor by an O-ring belt, which allowed a continuous range of velocities from 0 to 10 cm/sec. Two cams were used during this experiment—cam *A* generated a triangular velocity distribution (i.e., constant acceleration) and cam *B* generated a square velocity distribution (i.e., constant velocity).

Cam *A* was used as a “hunting” cam since the velocity distribution was divided into nine sectors between $+v_{\max}$ and $-v_{\max}$ and the counting rate could be recorded during one revolution for each interval. This cam was used to find the approximate width of the line and the magnitude of the effect to be expected.

Cam *B* was used to obtain details of the line shape because of the higher velocity resolution of 5%. The cam was divided into four sectors: $+v$, 0, $-v$, 0, and the counting rates for the two zero-velocity sectors were lumped together.

The electronic instrumentation for detection of the 71-keV gamma consisted of standard components. A ($1\frac{1}{2}$ in. \times 1 in.) NaI(Tl) crystal was mounted on a DuMont 6292 photomultiplier tube. The output signal was fed into a linear amplifier and a single-channel analyzer. The 71-keV line was in turn fed into one of a series of scalars. A particular scalar was singled out by one of a set of mercury switches synchronized with the cam rotation. Scalars counting a 60-cps pulse were placed in parallel with the counting rate scalars in order to record the time a particular velocity channel was open.

IV. MEASUREMENTS

Mössbauer measurements have been done until now with radioactive isotopes having half-lives of at least several days. The 99-min activity of Co^{61} requires either to measure the counting rates at different velocities simultaneously (cam *A*) or to take into account the decay by using the formula

$$M(v) = 1 - \frac{[R(v) - R(0)]}{e^{-\lambda t}[R(\infty) - R(0)]_{t=0}} \quad \lambda = \frac{\ln 2}{99 \text{ min}}, \quad (1)$$

where $R(v)$ is the counting rate at velocity v . Cam *B* gives directly $R(v)$ and $R(0)$ used in formula (1). The results of a systematic search at 41 velocities are shown in Fig. 4. The results given in Fig. 4 using Eq. (1) are

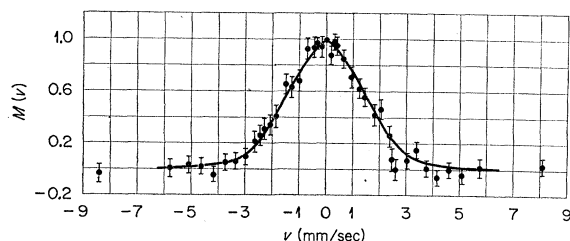


FIG. 4. The measured velocity dependence of the $M(v)$ for Ni^{61} is shown. The solid curve is a theoretical fit for $\mu_e = +1.15$ nm and $H = 61$ kgauss. The half-width is $(v^{\frac{1}{2}})_{\text{exp}} = 1.65$ mm/sec.

independent of the background. The absolute value of the resonance absorption effect requires, of course, careful investigation of the background. These corrections become more important as time progresses during a set of measurements, because of the relative fast decay of Co^{61} . The background to signal ratio b was determined by periodic measurements of the spectrum. Another effect which must be considered is the re-radiation r of the 71-keV gamma after absorption. The size of r depends on the geometry of the experiment and is in our case, 0.40. With this background taken into account we obtain for the absolute value of the Mössbauer effect:

$$\mathfrak{M}(v) = 2(1+r)(1+b) \times \left\{ \frac{R(\infty) - R(0)}{R(\infty) + R(0)} - \frac{R(v) - R(0)}{R(v) + R(0)} \right\}. \quad (2)$$

Figure 5 shows $\mathfrak{M}(0)$ as a function of the foil thick-

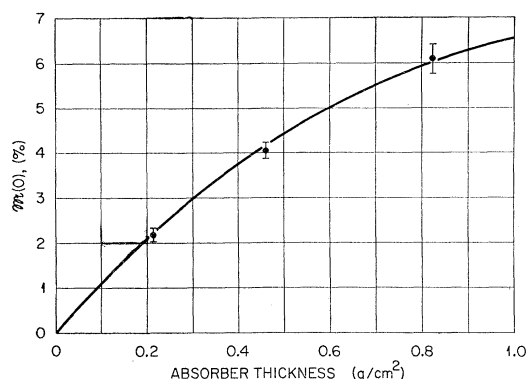


FIG. 5. The effect $\mathfrak{M}(0)$ at $T = 80^\circ\text{K}$ is shown for three foil thicknesses. The solid curve is a fit using Eq. (4) with $f = f' = 9\%$.

ness for a constant temperature $T = 80^\circ\text{K}$. Figure 6 demonstrates the temperature dependence of the effect for a constant thickness. The ordinate, f^2 , of Fig. 6 is related to $\mathfrak{M}(0)$ by the expression (5) given in the following section.

The measurement of the T dependence was carried out in the following way: The Dewar flask was filled with liquid nitrogen and the source and absorber were cooled to approximately 78°K . The liquid nitrogen was then removed from the Dewar and replaced by an atmosphere of dry nitrogen gas. The time required for the copper chamber to reach room temperature was several hours so that the temperature change during the time required to measure one point (~ 5 min) was small. The temperature was monitored regularly at intervals of five minutes.

V. DISCUSSION

Nuclear physics. The lifetime of the 71-keV Ni^{61} state, unknown during our measurements, was very recently

determined by Schwarzschild³ using a standard electronic method: $T_{\text{mean}} = (7.6 \pm 0.7) \times 10^{-9}$ sec. The internal conversion coefficient $\alpha = 0.12$ is known. A single line (without hyperfine structure splitting) in emission and absorption leads to a Lorentz-shape velocity dependence of the Mössbauer effect:

$$M(v) \propto \frac{1}{[v^2 + (v_{\frac{1}{2}})_{\text{nat}}^2]}, \quad \text{with} \\ (v_{\frac{1}{2}})_{\text{nat}} = \frac{c}{\omega_0 T_{\text{mean}}} = (0.37 \pm 0.036) \text{ mm/sec.}$$

The observed v -dependence (Fig. 4) has no Lorentz shape and has a half-width velocity $(v_{\frac{1}{2}})_{\text{exp}} = 1.65$ mm/sec. To understand this result, we assume a magnetic hyperfine structure splitting in source and absorber,⁴ produced by an internal magnetic field H .

The source and absorber consist of metallic Ni, so that $H_{\text{source}} = H_{\text{abs}} = H$. Later we have to average over all directions of H because we do not apply an external field.

The magnetic moment of the ground state, $\mu_g = (0.30 \pm 0.02)$ nm, was measured recently.⁵ The sign is probably negative (shell model). The magnetic moment μ_e of the excited state is unknown. The γ transition is $M1 + E2$. The $B(E2)$ -matrix element is known from Coulomb excitation,⁶ and the half-life, calculated with the $B(E2)$, is 1.2×10^{-6} sec. The measured mean life of 7.6×10^{-9} sec indicates therefore an almost pure $M1$ transition. The selection rule $\Delta m = \pm 1, 0$ yields then 12 different lines in the emission spectrum.

To get the line intensities and polarizations, one has to sum over all directions of H , or, somewhat simpler, to average over all γ -ray directions, keeping the field direction constant. Our measurements indicate that the distance between two adjacent lines is smaller than the natural linewidth. The interference terms between different lines vanish, the emitted γ rays are unpolarized. The emission spectrum $\epsilon(\omega)$ contains therefore 12 unpolarized slightly separated lines. The absorption probability of thin absorbers moving with a velocity v is proportional to $\epsilon(\omega + \omega_0 v/c)$. The Mössbauer effect $M(v)$ becomes

$$M(v) = M(-v) \propto \int_{-\infty}^{+\infty} \epsilon(\omega) \epsilon\left(\omega + \frac{v}{c} \omega_0\right) d\omega; \\ \omega_0 = E_\gamma / \hbar = \text{const.}$$

The integrand contains 144 terms, many of them are equal except for constant factors. Only 35 terms are really different (Appendix). We expect therefore 35 "unresolved" Mössbauer lines symmetrically to $v = 0$.

³ A. Schwarzschild (private communication).

⁴ There is no electric quadrupole splitting, because of the cubic symmetry of the Ni-lattice.

⁵ J. Orton, P. Auzins, and J. Wertz, Phys. Rev. **119**, 1691 (1960).

⁶ L. Fagg, E. Geer, and E. Wolicki, Phys. Rev. **104**, 1073 (1956).

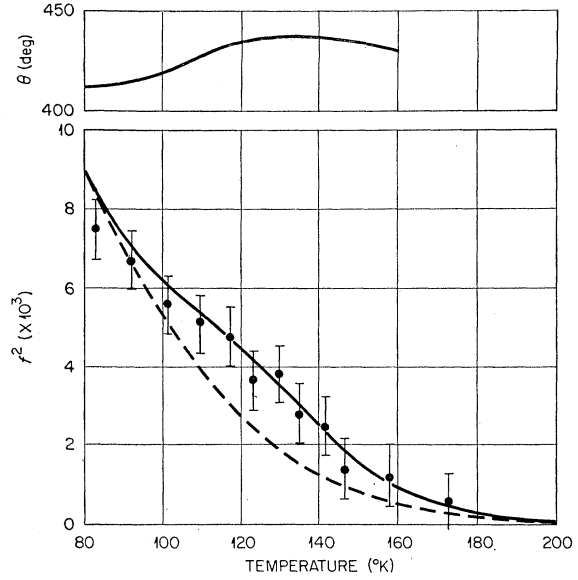


FIG. 6. The temperature dependence of $f^2 \propto \mathcal{M}(0)$. The dashed curve is obtained from the Debye model with $\theta = 413^\circ$. If θ is allowed to be slightly temperature dependent, as shown in the insert, then one gets the solid curve.

$M(v)$ depends on the known quantities T_{mean} , E_γ , μ_g , and the unknown parameters μ_e and H . In Fig. 4 we have fitted our experimental data points with $\mu_e = +1.15$ nm, $H = 61$ kgauss (solid line). There exists a set of μ_e - H values in agreement with the measurements. In Fig. 7 these values are plotted as a μ_e - H diagram. As was pointed out, the excited state is probably a $(f_{\frac{1}{2}})^1$ single-particle neutron state. The magnetic moment μ_e is then positive, which excludes the dashed branch in Fig. 7, if the sign of μ_g is really negative. The magnetic moments of all known odd-neutron states lie below the upper Schmidt-line,⁷ which gives in our case $0 \leq \mu_e \leq (5/7)|\mu_{\text{neutron}}|$. The internal magnetic field H corresponding to these limits lies between 55 and 220 kgauss.⁸

Solid-state physics. Consider the probabilities f and f' for recoil free gamma emission and absorption in the source and absorber. In the Debye model⁹ one gets

$$f = f' = \exp\{-0.75 E_\gamma^2 [1 + 6.6(T/\theta)^2] / M c^2 k \theta\}, \quad (3)$$

where θ = Debye temperature. To obtain f and f' from our measurements, we have to consider the absorber thickness and temperature dependence of $\mathcal{M}(v)$.

Given a spectrum with N lines, separated by an average distance Δ , each line with a natural line width Γ . If $\Delta \ll \Gamma$ but $N\Delta \gg \Gamma$, one gets an emission spectrum $\epsilon(\omega)$ with a rectangular shape:

$$\epsilon(\omega) = 1/2a \quad \text{for } |\omega - \omega_0| < a \\ = 0 \quad \text{for } |\omega - \omega_0| > a.$$

⁷ R. J. Blin-Stoyle, Revs. Modern Phys. **28**, 75 (1956).

⁸ A recent measurement of the internal magnetic field in nickel by the nuclear magnetic resonance method yields $H_{\text{int}} = 170$ kgauss at room temperature. L. Bruner, J. Budnick, and R. Blume, Phys. Rev. **121**, 83 (1961).

⁹ R. L. Mössbauer, Z. Physik **151**, 124 (1958).

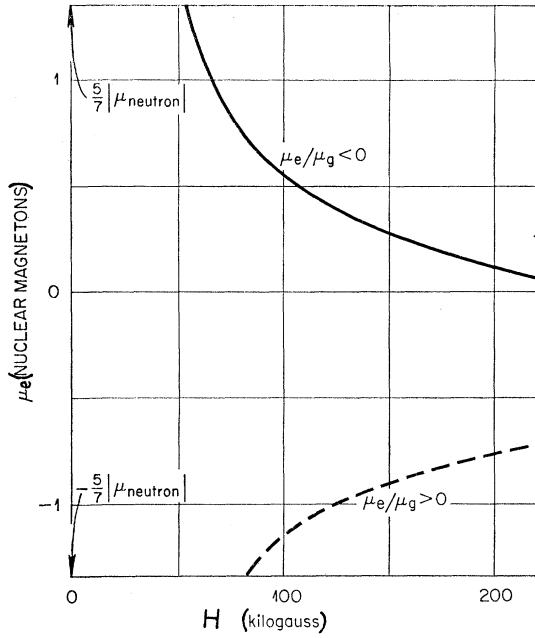


FIG. 7. The data points of Fig. 4 can be fitted with different values of the unknown parameters μ_e and H . The curves indicate possible values. The dashed curve is excluded by the shell-model prediction $\mu_e/\mu_g < 0$.

This condition is more or less fulfilled in the Ni^{61} case. A straightforward calculation yields the following results: The Mössbauer spectrum $\mathfrak{M}(v)$ is a triangle for all absorber thicknesses d (=number of Ni^{61} atoms/ cm^2). The half-width velocity $(v_{\frac{1}{2}})_{\text{exp}}$ of the triangle is independent of d and is connected with a by $(v_{\frac{1}{2}})_{\text{exp}} = c\alpha/\omega_0$. The thickness dependence of $\mathfrak{M}(v=0)$ is given by

$$\mathfrak{M}(0) = f \left[1 - \exp \left\{ -\frac{d\sigma_0 f'}{2} \frac{\pi (v_{\frac{1}{2}})_{\text{nat}}}{2 (v_{\frac{1}{2}})_{\text{exp}}} \right\} \right], \quad (4)$$

with

$$\sigma_0 = 2\pi\lambda^2 \frac{2I_e + 1}{2I_g + 1} \frac{1}{1 + \alpha}.$$

In Eq. (4) everything is known except f and f' . The values $f = (9.5_{-1.0}^{+1.5})\%$ and $f' = (8.0_{-2.0}^{+1.3})\%$ fit the measured d dependence in Fig. 5. This result indicates that $f' \cong f \cong (9 \pm 1)\%$ for $T = 80^\circ\text{K}$.

From Eq. (4) we get, with $f' = f$, for thin absorber foils

$$f^2 = \frac{4 (v_{\frac{1}{2}})_{\text{nat}}}{\pi\sigma_0 d (v_{\frac{1}{2}})_{\text{exp}}} \mathfrak{M}(0). \quad (5)$$

In Fig. 6 we have plotted the measured f^2 versus T . On the other hand, we can calculate f^2 in the Debye model Eq. (3). With $\theta = 413^\circ$ (taken from specific heat measurements) we get the dashed line. The solid line follows from a slightly temperature-dependent Debye temperature $413^\circ \leq \theta(T) \leq 437^\circ$. This T dependence of θ indicates the limit of the simple Debye model.

ACKNOWLEDGMENTS

We acknowledge with pleasure the benefit of the helpful discussions with various members of the Physics Division. We also wish to express appreciation to members of the staff shop and the ORNL 86-in. cyclotron crew.

APPENDIX

We have to investigate the influence of the hyperfine structure splitting on the Mössbauer effect. Take the internal field H in the z direction. An $M1$ transition from $I_e m_e$ to $I_g m_g$ (angular momenta of the excited and the ground state) leads to the frequencies

$$\omega(m_e \rightarrow m_g) = \omega_0 + \left(\frac{m_e}{I_e} \mu_e - \frac{m_g}{I_g} \mu_g \right) \frac{H}{\hbar}.$$

The angular distribution of the emitted γ rays with a polarization $\lambda = \pm 1$ (right- or left-hand screws) for this transition is given by

$$W(m_e \rightarrow m_g) \propto \sum_{q=-1}^{+1} \begin{pmatrix} I_e & I_g & 1 \\ m_e & -m_g & q \end{pmatrix}^2 |V_{-q}(\lambda; \vartheta, \varphi)|^2,$$

with $V_0 = \sin\theta$ and $V_{\pm 1} = \pm e^{\pm i\varphi} (\cos\theta - \lambda)/\sqrt{2}$.

To get the transition intensities $I(m_e \rightarrow m_g)$, one has to integrate $W(m_e \rightarrow m_g)$ over $d\Omega$ because the internal field direction is distributed randomly. The result,

$$I(m_e \rightarrow m_g) \propto \begin{pmatrix} I_e & I_g & 1 \\ m_e & -m_g & m_g - m_e \end{pmatrix}^2,$$

is independent of the polarization λ .

Every hyperfine structure line has, of course, a Lorentz shape with a half-width $\Gamma = \hbar/T_{\text{mean}}$. The emission spectrum $\epsilon(\omega)$ is the sum over all lines:

$$\epsilon(\omega) \propto \sum_{m_e, m_g} \begin{pmatrix} I_e & I_g & 1 \\ m_e & -m_g & m_g - m_e \end{pmatrix}^2 \times \frac{[\Gamma/2\hbar]^2}{[\omega - \omega(m_e \rightarrow m_g)]^2 + [\Gamma/2\hbar]^2}.$$

The Mössbauer effect for thin absorber foils is

$$\begin{aligned} M(v) &\propto \int_{-\infty}^{+\infty} \epsilon(\omega) \epsilon\left(\omega + \frac{v}{c} \omega_0\right) d\omega \\ &\propto \sum_{m_g, m_g'} \sum_{m_e, m_e'} \begin{pmatrix} I_e & I_g & 1 \\ m_e & -m_g & m_g - m_e \end{pmatrix}^2 \\ &\quad \times \begin{pmatrix} I_e & I_g & 1 \\ m_e' & -m_g' & m_g' - m_e' \end{pmatrix}^2 \\ &\quad \times \frac{4}{[x + (m_e - m_e')p - (m_g - m_g')q]^2 + 4} \equiv N(x; p, q), \end{aligned}$$

where

$$x = 2(v/c)(E_\gamma/\Gamma), \quad p = 2\mu_e H/I_e \Gamma, \quad q = 2\mu_g H/I_g \Gamma,$$

and

$$N(x; p, q) = N(-x; p, q) = N(x; -p, -q), \quad N(0; 0, 0) = 1.$$

For Ni^{61} ($I_e = \frac{5}{2}$, $I_g = \frac{3}{2}$) one gets 35 different pairs of

$(m_e - m_e')$ and $(m_g - m_g')$ values, that is, a combination of 35 Mössbauer lines. The unknown parameters are H and μ_e or p and q . We have written a code for the ORACLE computer, which yields $N(x)$ for fixed p and q values in the form of a curve. Many of these curves have the measured half-width $x_{\frac{1}{2}} = 2E_\gamma(v_{\frac{1}{2}})_{\text{exp}}/c\Gamma = 8.75$ and a shape in agreement with our measurements (one typical case is shown in Fig. 4).

Electron Spin-Lattice Relaxation of Chromium in MgO^\dagger

J. G. CASTLE, JR., AND D. W. FELDMAN
Westinghouse Research Laboratories, Pittsburgh, Pennsylvania

(Received October 31, 1960)

The effective spin-lattice relaxation time, T_1 , has been observed for the ground-state multiplet of $\text{Cr}(+3)$ in the cubic field of MgO . T_1 is observed to vary from 800 milliseconds at 1.3° to 3.4 milliseconds at 50°K . The direct process dominates below 4.2° .

SPIN relaxation within the ground-state multiplet of the chromium $(+3)$ ion has been of interest for some time.¹⁻⁸ We have observed the spin-lattice relaxation of $\text{Cr}(+3)$ in the cubic environment of MgO from 1.3°K to 50°K . For this case, i.e., a multiplet having equally spaced energy levels and therefore a common spin temperature, a unique spin-lattice time is expected and was found in very dilute samples. The general problem of spin relaxation in MgO at even moderate concentrations is complicated apparently by the existence of other impurities.

The paramagnetic resonance spectra of $\text{Cr}(+3)$ substituted for $\text{Mg}(+2)$ in MgO have been clearly shown⁹ to be due to some chromium ions in a cubic environment and to others having an $\text{Mg}(+2)$ vacancy nearby. On the basis of charge neutrality, the concentration of excess $\text{Mg}(+2)$ vacancies is expected to be at least half that of trivalent impurities. Apparently, a considerable fraction of the trivalent impurities are closely associated with $\text{Mg}(+2)$ vacancies. The central line from a $\text{Cr}(+3)$ -[100] vacancy pair lies about 2 gauss above the cubic chromium line at 9 kMc/sec with H along [100].

The microwave spectra of the other transition ele-

ments in MgO have been reported.^{9,10,11} The crystals being used in the present study show absorption by $\text{Cr}(+3)$, $\text{Fe}(+3)$, $\text{Mn}(+2)$, $\text{V}(+2)$, and $\text{Fe}(+2)$ in a cubic environment, and $\text{Cr}(+3)$ -vacancy pairs. At 9 kMc/sec, one of the $\text{Mn}(+2)$ $(-\frac{1}{2}-\frac{1}{2})$ lines is about one gauss below the cubic chromium line, the $(-\frac{1}{2}-\frac{1}{2})$ line of $\text{Fe}(+3)$ with H along [100] is about 50 gauss below, and the central pair of $\text{V}(+2)$ lines are split to about 40 gauss each side of the cubic chromium line. The $\text{Fe}(+2)$ line at 1800 gauss¹⁰ was observed only in some of the samples which had higher chromium concentration. Spectrographic analysis showed impurity concentrations (other than for chromium) to be of the order of 10 parts per million (ppm), with Fe consistently higher than the others.

Using the inversion-recovery method previously described,⁴ the spin population difference, n , is observed directly as a function of time after inversion by adiabatic fast passage. When recovery of equilibrium for $S = \frac{1}{2}$ is dominated by spin-lattice relaxation, the deviation of n from its equilibrium value is expected to vary as $\exp(-t/T_1)$, where T_1 is the spin-lattice relaxation time. This single exponential recovery is also expected for $\text{Cr}(+3)$ in the cubic environment of MgO . Conversely, the observation of nonexponential recovery of the cubic chromium line implies that other relaxation processes are operative.

Exponential recovery of the cubic $\text{Cr}(+3)$ line was observed in two of the purest crystals available as a function of temperature up to 50°K ; the values of T_1 so obtained are listed in Table I. For spin-lattice relaxation by resonant phonons¹ at frequency f , T_1

[†] These studies were supported by the Air Force Research Division.

¹ J. H. Van Vleck, *Phys. Rev.* **57**, 426 (1940); **59**, 724 (1941).

² S. Shapiro and N. Bloembergen, *Phys. Rev.* **116**, 1453 (1959).

³ R. D. Mattuck and M. W. P. Strandberg, *Phys. Rev.* **119**, 1204 (1960).

⁴ J. G. Castle, P. F. Chester, and P. E. Wagner, *Phys. Rev.* **119**, 953 (1960).

⁵ J. H. Pace, D. F. Sampson, and J. S. Thorp, Royal Radar Establishment Memo 1693, January, 1960 (unpublished).

⁶ R. Michel, *J. Phys. Chem. Solids* **13**, 164 (1960).

⁷ J. E. Geusic, *Phys. Rev.* **118**, 129 (1960).

⁸ N. S. Shiren, *Bull. Am. Phys. Soc.* **5**, 343 (1960).

⁹ J. E. Wertz and P. Auzins, *Phys. Rev.* **106**, 484 (1957).

¹⁰ W. Low, *Phys. Rev.* **101**, 1827 (1956); **118**, 1608 (1960).

¹¹ J. H. E. Griffiths and J. W. Orton, *Proc. Phys. Soc. (London)* **73**, 948 (1959).